Pharmacogn. Mag.
A multifaceted peer reviewed journal in the field of Pharmacognosy and Natural Products
www.phcog.com | www.phcog.net

ORIGINAL ARTICLE

Structural Characterization and Immune Regulation of a New Heteropolysaccharide from *Catathelasma imperiale* (Fr.) Sing

Lu Liu[1], Xiang Ding[1,2], Yiling Hou[1]

[1]Key Laboratory of Southwest China Wildlife Resources Conservation (Ministry of Education), College of Life Sciences, China West Normal University, [2]College of Environmental Science and Engineering, China West Normal University, Nanchong, Sichuan Province, China

Submitted: 03-01-2019 Revised: 12-02-2019 Published: 19-09-2019

ABSTRACT

Background: Polysaccharide has played the part of great role in pharmacology and physiology. **Materials and Methods:** In this study, the polysaccharides (CIS-A) from *Catathelasma imperiale* (Fr.) Sing, were isolated and purified by hot water extraction technology and column chromatography, respectively. Chemical methods, infrared spectrum, high-performance gel-permeation chromatography, high-performance liquid chromatography, gas chromatography–mass spectrometry, ^{1}H nuclear magnetic resonance spectroscopy (NMR), ^{13}C NMR, and two-dimensional NMR were used to characterize the polysaccharides of CIS-A. The anticancer and immunomodulatory ability of the polysaccharides (CIS-A) from the fruiting body of *C. imperiale* (Fr.) Sing was also investigated. **Results:** The structural feature analysis showed the polysaccharide (CIS-A) which had a molecular weight of 50486 Da was mainly composed of α-D-glucose pyranose (α-D-Glcp) and β-L-fucose pyranose (β-L-Fucp). It had a backbone of three 1, 3-linked α-D-Glcp. There is a branch at the C2 of the polysaccharide backbone. The branches were mainly composed of two 2, 3-linked β-L-Fucp residue. Antitumor activity results showed that CIS-A could inhibit the growth of S180 tumor and promote the apoptosis of L929 cells. Immunoregulatory activity results showed that CIS-A could promote the proliferation of T-cells and promote B-cells by affecting G0/G1 phase, S phase, and G2/M phase. It also could promote the proliferation and phagocytosis of macrophages and induce cytokine release. **Conclusion:** Polysaccharide CIS-A can be used as a candidate drug for antitumor and immunomodulator.

Key words: Biological activity, immune regulation, polysaccharide, structure elucidation, Xiaojin *Catathelasma imperiale* (Fr.) Sing

SUMMARY

- A new polysaccharide (CIS-A) was purified and identified from *Catathelasma imperiale* (Fr.) Sing for the first time
- The polysaccharide (CIS-A) had a molecular weight of 50486 Da was mainly composed of α-D-glucose and β-L-fucose
- CIS-A could inhibit the growth of S180 tumor and promote the apoptosis of L929 cells
- CIS-A could promote the proliferation of T-cells and B-cells
- CIS-A could promote the proliferation and phagocytosis of macrophages and induce cytokine release.

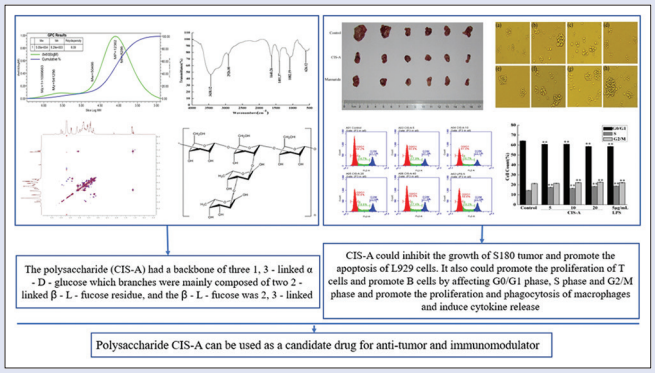

Abbreviations used: CIS-A: The polysaccharides from *Catathelasma imperiale* (Fr.) Sing; IR: Infrared spectrum; HPGPC: High-performance gel-permeation chromatography; HPLC: High-performance liquid chromatography; GC-MS: Gas chromatography–mass spectrometry; ^{1}H NMR: ^{1}H nuclear magnetic resonance spectroscopy; ^{13}C NMR: ^{13}C nuclear magnetic resonance spectroscopy; 2D NMR: Two-dimensional nuclear magnetic resonance spectroscopy; TFA: Trifluoroacetic acid.

Correspondence:

Prof. Yiling Hou,
Key Laboratory of Southwest China Wildlife Resources Conservation, College of Life Sciences, China West Normal University, No. 1, Shida Road, Nanchong, Sichuan Province 637009, China.
E-mail: starthlh@126.com

DOI: 10.4103/pm.pm_673_18

Access this article online
Website: www.phcog.com
Quick Response Code:

INTRODUCTION

The polysaccharide is composed of at least ten monosaccharides, and they were linked together by glycosidic bond.[1] Polysaccharides have played the part of great role in pharmacology and physiology. They act as barriers between the cell wall and the environment and have the function of mediating the host–pathogen interaction and forming biofilm structure. In recent years, active polysaccharides have been widely concerned because of their immunomodulatory, antitumor, antiviral, antioxidant, and hypoglycemic effects.[2,3] At the same time, active polysaccharide can be multichannel, multilink, multitarget regulation of the immune system, activation of immune cells, and activation of complement and promote the formation of cytokine. A wide range of fungal polysaccharides, which sources of raw materials are simple, have a unique role in medicine, agriculture, food, and other fields.

In this study, the polysaccharides from *Catathelasma imperiale* (Fr.) Sing (CIS-A) were isolated and purified by hot water extraction technology and column chromatography, respectively.[4,5] Chemical methods, infrared spectrum (IR), high-performance gel-permeation chromatography (HPGPC), high-performance liquid

Cite this article as: Liu L, Ding X, Hou Y. Structural characterization and immune regulation of a new heteropolysaccharide from *Catathelasma imperiale* (Fr.) Sing. Phcog Mag 2019;15:621-30.

chromatography (HPLC), gas chromatography–mass spectrometry (GC-MS), ^{1}H nuclear magnetic resonance spectroscopy (NMR), ^{13}C NMR, and two-dimensional NMR were used to characterize the polysaccharides of CIS-A. The anticancer and immunomodulatory ability of the polysaccharides (CIS-A) from the fruiting body of *C. imperiale* (Fr.) Sing was also investigated. This study provided scientific basis for the further study on the pharmacological action, structure–activity relationship, and more extensive application of fungal polysaccharide (CIS-A).

MATERIALS AND METHODS

Chemicals

Fresh fruiting bodies of *C. imperiale* (Fr.) Sing were collected from Xiaojin County which lies in the Sichuan Aba Tibetan and Qiang Autonomous Prefecture. After vacuum freeze-drying, it was crushed and stored at 4°C for use in the Key Laboratory of Southwest China Wildlife Resources Conservation, College of Life Sciences, China West Normal University, China. The ethanol was purchased from Swancor (Shanghai Fine Chemical Co., Ltd. (Shanghai, China). Sodium chloride was purchased from Sichuan Kelun Pharmaceutical Co., Ltd. (Chengdu, China). Trifluoroacetic acid (TFA), the standard monosaccharide, and dextran of different molecular weights were purchased from Tianjin Kermel Chemical Reagent Co., Ltd. (Tianjin, China). Diethylaminoethyl (DEAE)-cellulose column, Sephacryl S-300 gel column, and Sephadex G-200 column were purchased from Beijing Solarbio Science and Technology Co., Ltd. (Beijing, China). Cell counting kit-8 (CCK-8) was purchased from Dojindo Molecular Technologies, Inc., (Shanghai, China). Phosphate-buffered saline (PBS) buffer, RPMI1640 medium, phenol red free, 0.5% trypsin-ethylenediaminetetraacetic acid, and fetal bovine serum were available from Thermo Fisher Scientific Inc. (New York, USA). All analytical reagents were of analytical grade.

Extraction of polysaccharides from *Catathelasma imperiale* (Fr.) Sing

The fresh fruiting bodies of *C. imperiale* (Fr.) Sing were thoroughly washed with water, dried at 60°C, and pulverized by a pulverizer. For conventional extraction, 300 g fruiting body was accurately weighed as dry and powdery. The powder was boiled in boiling water for 6 h at the ratio of 1:3.[6] After boiling the powder three times, the supernatant was collected and evaporated to 300 mL. Four volumes of absolute ethanol were added to precipitate crude polysaccharide. Flocculent precipitation which generated by stirring with glass rods was collected by centrifugation. 5 mg of the accurately weighed crude polysaccharide was dissolved in 5 mL of distilled water.[7] The supernatant was added to DEAE-cellulose-52 column (2 cm × 60 cm). Different concentrations of NaCl (0 mol/L, 0.1 mol/L, 0.2 mol/L, 0.3 mol/L, 0.4 mol/L, and 0.5 mol/L) were prepared as mobile elution phase elution. The polysaccharide was determined by phenol–sulfuric acid method.[8] The eluate in the distilled water was purified on Sephadex G-200 and then concentrated. The small molecule compound was removed by dialysis (7 kDa) for 48 h. *C. imperiale* (Fr.) Sing polysaccharide, named CIS-A, was obtained by vacuum lyophilization for further analysis of the structure.

Molecular weight determination of polysaccharide CIS-A

5 mg of the CIS-A polysaccharide sample was dissolved in 3 mL of double-distilled water, sonicated for 5 min, and then filtered with a filter (0.22 μm). The molecular weight of CIS-A was determined by HPGPC.[9] The measured data were subjected to GPC software (Agilent GPC Data Analysis Software for Agilent ChemStation, Agilent Technologies Inc., Beijing, China) with a standard curve prepared from dextran to obtain molecular weight.

Fourier-transform infrared spectrometer analysis

The working principle of infrared spectroscopy is due to different vibration levels. The resonant frequency depends on the shape of the equipotential surface of the molecule, the atomic mass, and the final correlation of the vibrational coupling. 5 mg of CIS-A was mixed with KBr powder and then pressed and scanned in the Fourier-transform infrared spectrometer (FT-IR) at a range of 4000 cm^{-1} to 400 cm^{-1}.[10]

Monosaccharide composition analysis of CIS-A

20 mg of the CIS-A polysaccharide was dissolved in 5 mL 2 mol/L TFA. The solution were sealed to hydrolyze for 6 h at 90°C.[11,12] The supernatant was centrifuged and extracted with chloroform. The hydrolysate was obtained by lyophilization. Monosaccharide composition analysis of CIS-A was done by HPLC (Agilent Technologies Inc., Beijing, China). The chromatographic conditions were as follows: 4.6 mm × 250 mm, 5 μm column; column temperature: 25°C; mobile phase: 75% acetonitrile; flow rate: 1.4 mL/min; Refractive index detector temperature: 35°C; and injection volume: 5 μL.[13]

Nuclear magnetic resonance experiment

20 mg of CIS-A was weighed and dissolved in D_2O.[14] The Varian Unity INOVA 400/45 (Varian Medical Systems, Inc., California, USA) was used to perform the ^{1}H NMR spectral and ^{13}C NMR spectral analysis with tetramethylsilane as internal standard.[15]

Methylation analysis and gas chromatography–mass spectrometry

Methyl iodide was used to prepare polysaccharide methylation.[16] The methylated product was dried. The methylated product was dried and dissolved in 2M TFA and hydrolyzed at 100°C for 6 h. The resulting hydrolyzate was derivatized using a silylating reagent and analyzed by GC-MS. The temperature program was set as follows: the initial temperature was maintained at 80°C for 3 min and then raised to 200°C at a rate of 10°C/min and maintained at 200°C for another 10 min.

Animals

The mice were Kunming mice from the Institute of Biochemistry and Molecular Immunology, North Sichuan Medical College. Male Kunming mice weighing 25.0 ± 1.0 g were housed in plastic cages. They were given 12 h of light and 12 h of darkness per day and allowed to eat freely. Experimental program was approved by the North Sichuan Medical College.

Assay of antitumor activity *in vivo*

S180 tumor cells (3×10^6) were injected into the right posterior abdomen of Kunming male mice.[8] Mice were randomly divided into four groups ($n = 6$): blank control group (without injecting S180 cells), S180-control group (injecting S180 cells), polysaccharide CIS-A group (injecting S180 cells and 20 mg/kg of polysaccharide CIS-A) and positive control group (injecting S180 cells and 20 mg/kg mannatide), respectively. The mice were sacrificed 2 weeks later. The tumor, spleen, and liver were resected. The tumor inhibition rate was calculated by the following formula: inhibition rate (%) = ([A − B]/A) × 100, where A was the average tumor weight of S180-control group and B was the average tumor weight of medicine groups.[17]

Cell lines and reagents

L929 cell line, T-cell line, B-cell line, and RAW264.7 cell line were cultured in a cell culture medium (10% fetal bovine serum, 1% penicillin (100 IU/mL), streptomycin (100 mg/L), and RPMI 1640 medium) in an incubator at 5% CO_2, 37°C.

Pharmacological evaluation for T-cell, B-cell, and RAW264.7 cell stimulation and L929 cell growth inhibition

Pharmacological evaluation for T-cell, B-cell, and RAW264.7 cell stimulation and L929 cell growth inhibition was tested by CCK-8.[18] On the 1st day, cells cultured in RPMI-1640 medium at a density of 1×10^5 cells/mL were added to 96-well plates at 100 μl per well and incubated in a 5% CO_2 incubator for 24 h at 37°C.[15] On the 2nd day, the cell culture medium with different concentrations of CIS-A (1.25, 2.5, 5, 10, 20, and 40 μg/mL in T-cell, B-cell and RAW264.7 cell groups and 0.625, 1.25, 2.5, 5, 10, and 20 μg/mL in L929 cell group) were added to 96-well plates. 5 μg/mL lipopolysaccharide (LPS) was used as positive control, and the cell culture medium without CIS-A was used as blank control. After incubated at 37°C for 24 h, 10 μL of CCK-8 reagent was added to each well and further incubated for 2–4 h. The absorbance of the colored solution at 450 nm was measured on a 96-well microplate reader. Cell viability was calculated as follows: Cell viability (%) = ([Ac − As]/[Ac − Ab]) × 100%, where Ac was the absorbance of control group, Ab was the absorbance of blank group, and As was the absorbance of experimental group.

Effects of CIS-A on B-cell cycle

B-cells were suspended in the culture bottle, and B-cell cycle was detected by cell cycle and apoptosis detection kit. B-cell cycle test includes the blank control group, the experimental group (CIS-A: 5, 10, and 20 μg/mL), and the positive control group (LPS: 5 μg/mL). 1 mL of 70% ethanol was added to cell plates for cell immobilization at 4°C for 2 h. 0.5 mL of propidium iodide staining solution was added to each cell sample, and the cells were incubated at 37°C for 30 min. The absorbance value at 488 nm was measured on a flow cytometer, and the percentages of cells in each cell cycle (G0/G1 phase, S phase, and G2/M phase) were analyzed.[19]

Nitric oxide determination

RAW264.7 cells were stimulated with CIS-A polysaccharide for 24 h. Nitric oxide (NO) determination was done by Griess method.[20]

Pharmacological evaluation for macrophage phagocytic activity

RAW264.7 cells were cultured on 96-well plates (1×10^5 cells/mL) and incubated for 24 h. 100 μL of cell culture medium (blank control), LPS (final concentration 5 μg/mL, positive control), and the polysaccharide of CIS-A (0.625, 1.25, 2.5, 5, 10, and 20 μg/mL) were added to 96-well plates, respectively. After incubated at 37°C for 24 h, neutral red reagent (0.075 g/L) was added to 96-well plates. Moreover, after 30 min, the neutral red reagent was discarded, and the RAW264.7 cells were washed three times with PBS and then added 200 μL lysis buffer (glacial acetic acid: ethanol = 1:1). After incubated at 37°C for 2 h, the absorbance value at 540 nm was measured.

Statistical methods

All data in this study were analyzed by the way of standard deviation. Methods of data processing were one-way analysis of variance and Student's *t*-test. $P < 0.05$ represents a significant difference between the data.

RESULT AND DISCUSSION

Determination of molecular weight

Method for testing molecular weight of CIS-A was HPLC-GPC. The peaks of CIS-A polysaccharides on HPLC-GPC were broadly symmetrical. Figure 1a shows the high-performance gel-permeation chromatogram of CIS-A. The molecular weight (Mw) of CIS-A was 50486 Da, the peak molecular weight (Mp) was 12362 Da, the number average molecular weight (Mn) was 8286 Da, and the polydispersity was 6.09.

Fourier-transform infrared spectrometer analysis

The absorption peaks of CIS-A polysaccharides were not measured at wavelengths of 280 nm and 260 nm, indicating that the protein and nucleic acid impurities had been minimal. The FT-IR spectra of the purified CIS-A displayed typical absorption peaks of polysaccharides in the range of 4000–500 cm^{-1} [Figure 1b].

The structure of CIS-A was analyzed by FT-IR. A broad absorption peak at 3438.12 cm^{-1} was designated as OH stretching vibration peak, 2926 cm^{-1} was designated as CH stretching vibration peak, 1640.26 cm^{-1} was designated as CO stretching vibration peak, 1401.37 cm^{-1} was designated as bending vibration peak of CH_2, CH, and OH, 1082 cm^{-1} was designated as CO stretching vibration peak, and at the same time, 626.12 cm^{-1} was designated as C-H rocking vibration peak.[21]

Monosaccharide composition analysis

The polysaccharide CIS-A was hydrolyzed with TFA and analyzed for component monosaccharides by HPLC. Compared with the retention time of the standard monosaccharide, the peak at retention time of 7.149 min represented the glucose. In addition, there was a shoulder peak near the retention time of 7.149 min. The results of structural analysis showed that polysaccharides CIS-A were mainly composed of glucose [Figure 1c and d]. The monosaccharide configuration was consistent with GC-MS analysis.

Analysis of the nuclear magnetic resonance experiment results

The hydrogen spectrum of CIS-A was shown in Figure 1e. In the ^1H NMR (400 HZ) spectrum, δ5.00, δ4.91, and δ4.44 indicated that the polysaccharides CIS-A had three anomeric protons, which indicated that CIS-A consisted of at least two monosaccharides. The anomeric proton signal at δ4.44 was assigned to β-pyranose unit, whereas other signals at δ5.00 and δ4.91 were attributed to α-pyranose forms. The anomeric proton signal at δ1.17 was assigned to H-6 of β-L-Fucp.[22] The hydrogen signal for water was δ4.70. The signal peaks at δ3.23–δ4.46 were the signal peak of the remaining protons except the protons of CH_3 in the polysaccharide, which consisted of the multiple overlapping signal peaks.[23,24]

In the ^{13}C NMR spectra of CIS-A, the signals of δ101.46, δ102.95, and δ97.84 were anomeric carbon peaks, which indicated that the polysaccharides CIS-A had α- and β-anomeric configurations. The results were consistent with the analysis of IR and ^1H NMR. The chemical shift was not found in the region between δ160.00 and δ180.00, which indicated that there was no carboxyl in CIS-A. The signal of furan ring should be near δ106–δ109.[25] According to the literature,[26] the resonances in the region of δ97–δ104 in the ^{13}C NMR (400 MHz) spectrum of CIS-A were attributed to the anomeric carbon atoms of D-glucose pyranose (D-Glcp) and in the region of δ100–103 to the anomeric carbon atoms of L-fucose pyranose (L-Fucp), respectively. In addition, δ15.65 was assigned to C-6 of Fucp. In the anomeric carbon region, signal at δ101.46 could be attributed to

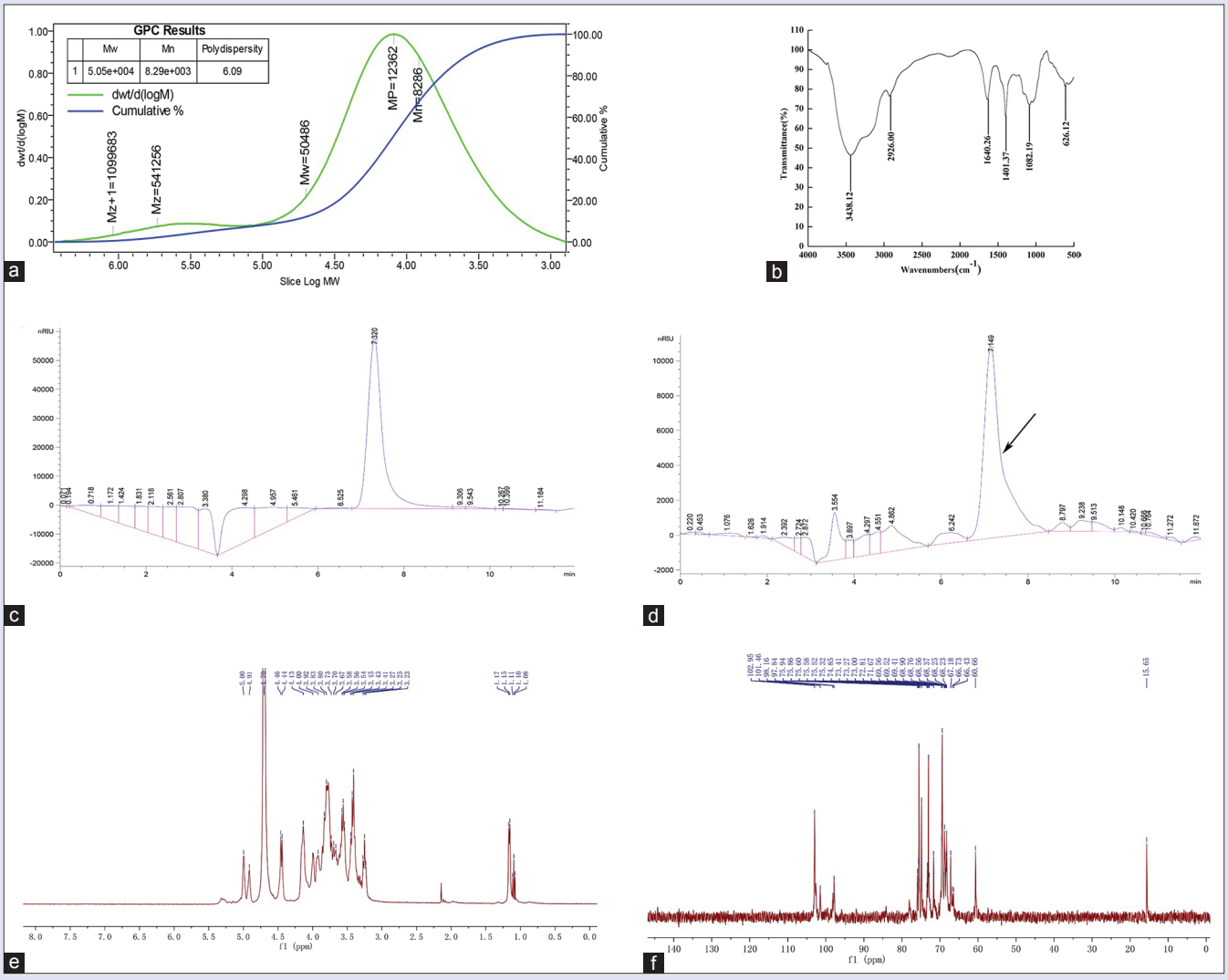

Figure 1: (a) The molecular weight of CIS-A, (b) Fourier-transform infrared spectra of CIS-A, (c) chromatography of glucose by high-performance liquid chromatography, (d) the component monosaccharide analysis of polysaccharides by high-performance liquid chromatography, (e) The ^{1}H nuclear magnetic resonance spectroscopy spectra of CIS-A, (f) the ^{13}C nuclear magnetic resonance spectroscopy spectra of CIS-A

C-1 of →3)-α-D-Glcp-(1→; signal at δ97.84 could be attributed to C-1 of →2,3)-α-D-Glcp-(1→; signal at δ102.95 could be attributed to C-1 of β-L-Fucp-(2→ [Figure 1f]. All the assignments of the carbon atom signals are shown in Table 1.

A proton chemical shift at δ5.00, δ4.91, and δ4.46 and a cross peak at 5.00/3.56, 4.91/3.77, and 4.44/3.25 ppm were readily obtained from H-H COSY [Figure 2a], which implied that the chemical shift of H2 was 3.56, 3.77, and 3.25 ppm, respectively. There was a cross peak at 4.13/1.17 ppm, which implied that the chemical shift of H5 was 4.13 ppm. Inspection of the heteronuclear multiple quantum coherence (HMQC) spectrum [Figure 2b] showed that the H1 tracks a close connectivity with C1 in agreement with H1/C1 (4.44/102.95 ppm), H1/C1 (5.00/101.46 ppm), and H1/C1 (4.91/97.84 ppm) in the anomeric atom region. Moreover, there was a cross peak at H6/C6 (1.17/15.65 ppm), which was also the signal of fucose. Based on these proton chemical shifts, the carbon signals of C1–C6 could be found easily from HMQC and corresponded nearly to the documented reference values. The downfield shifts of C1 (101.46 ppm) and C3 (66.73 ppm), C1 (97.84 ppm) and C3 (72.94 ppm), and C1 (102.95 ppm) and C3 (75.52 ppm) confirmed the existence of 1,3-linked α-D-Glcp, →2,3)-α-D-Glcp-(1→ and →3)-β-L-Fucp-(2→, respectively, which consistented with the results of GC-MS analysis.

Table 1: ^{13}C nuclear magnetic resonance spectroscopy chemical shift data (δ, ppm) for polysaccharide CIS-A

Monosaccharide residues	Chemical shift, δ (ppm)					
	C1	C2	C3	C4	C5	C6
→3)-α-D-Glcp-(1→	101.46	66.43	66.73	69.56	75.32	68.23
→2,3)-α-D-Glcp-(1→	97.84	73.00	75.52	69.41	74.85	67.18
→3)-β-L-Fucp-(2→	102.95	68.23	72.94	68.76	72.81	15.65

δ: Chemical shift symbol; ppm: Parts per million; →: Linkage sites

The overlapping signals between carbons and protons were identified through the HMQC spectroscopy [Figure 2b] and available in the literatures. Considering all chemical signals, it could conclude the α-linked D-glucopyranose unit and β-linked L-6-deoxy-galactosepyranose (L-fucose) unit. The sequence of monosaccharide residues of CIS-A was analyzed by a long-range ^{1}H-^{13}C heteronuclear multiple bond

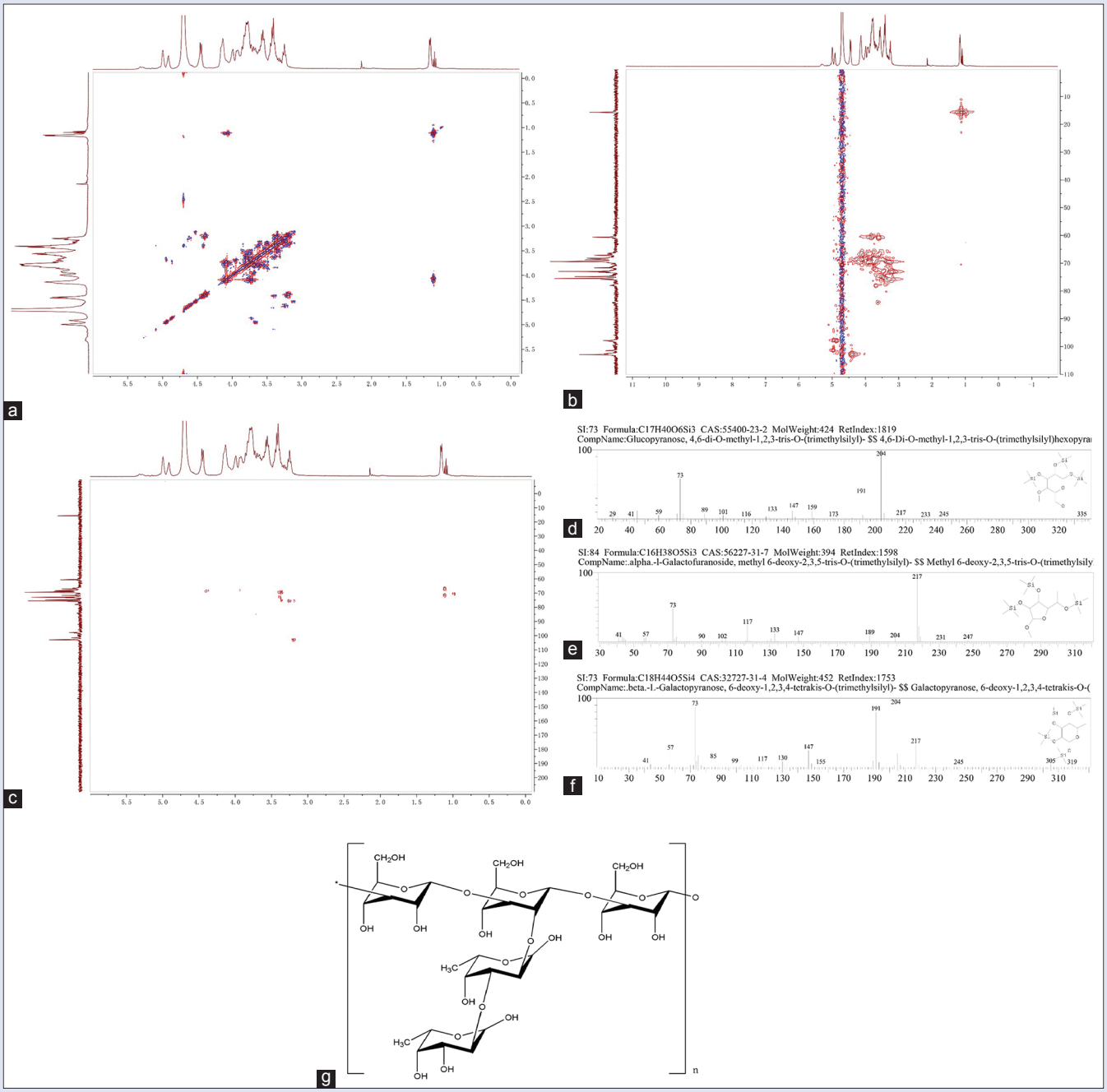

Figure 2: (a) H-H COSY spectrum of polysaccharide CIS-A, (b) heteronuclear multiple quantum coherence spectrum polysaccharide CIS-A, (c) heteronuclear multiple bond correlation spectrum polysaccharide CIS-A, (d) the fragment ion peaks of 1,2,3-tris-O-trimethylsily-Glc, (e) The fragment ion peaks of methyl 6-deoxy-2,3,5-tris-O-trimethylsily-Gal, (f) The fragment ion peaks of 6-deoxy-1,2,3,4-tetrakis-O-trimethylsily-Gal, (g) predicted chemical structure of polysaccharide CIS-A

correlation (HMBC) studies [Figure 2c]. Clear inter-residual HMBC correlations were found between →2,3)-α-D-Glcp-(1→ residue H1 and C3, →3)-α-D-Glcp-(1→ residue H1 and C3 and →3)-β-L-Fucp-(2 → residue H1 and C3, respectively. In according to these apparent assignments above, the characterized polysaccharide showed a main chain of →3)-α-D-Glcp-(1→ and were mainly composed of (2→3)-linked-β-L-fucose residue.

Moreover, all the above-mentioned chemical shifts and spectroscopic evidences also firmly supported →2,3)-α-D-Glcp-(1→ link site. Hence, on the basis of results from the monosaccharide composition, methylation analysis, NMR analysis, and GC-MS analysis, one of the possible preliminary structures of CIS-A was predicted.

Analysis of the gas chromatography–mass spectrometry experiment results

The methylated products of CIS-A were hydrolyzed with acid, converted into silane compound, and analyzed by GC-MS. Experiment data were settled and are listed in Table 2. The methylation analysis for CIS-A proved that the α-D-Glcp residues were 1, 2, 3-tris-O-trimethylsilyl-substituted and the β-L-Fucp residues were

methyl-6-deoxy-2, 3, 5-tris-O-trimethylsily-substituted and 6-deoxy-1, 2, 3, 4-tetrakis-O-trimethylsily-substituted [Figure 2d-f and Table 2]. In the course of experiment, there might be incomplete methylation. Results of methylated linkage analysis of CIS-A indicated that (1→3)-linked-α-D-Glcp was one of the largest amounts, residue of the polysaccharide structure. The branched residues were (2→3)-lin ked-β-L-6-deoxy-β-L-fucose pyranose (β-L-Fucp) revealing that (1→3, 2)-linked-α-D-Glcp should be also possible to form the backbone structure. Residues of branch structure were terminated with β-L-Fucp residues. It was concluded that a repeating unit of CIS-A had a backbone of (1→3)-α-D-Glcp and (1→3, 2)-α-D-Glcp. The branch was supposed to be the composition of two with (2→3)-β-L-fucose residues. The mole ratio of the glycosyl residues was calculated from the peak areas in the total ion chromatogram.

On the basis of the above experimental data, we elucidated the possible structure of CIS-A which had a backbone of 1, 3-linked-α-D-glucose and 1, 2, 3-linked-α-D-glucose. The branches were mainly composed of two (2→3)-linked-β-L-fucose residues [Figure 2g].

Antitumor activity of CIS-A

In this study, CIS-A was used to transplant S180 in mice to test their antitumor activity *in vivo*. The result showed that CIS-A could inhibit tumor growth. The inhibition rate of 20 mg/kg in treated mice was 64.4%. In this experiment, the appetite, activity, and fur surface gloss of mice in CIS-A group almost were as the same as mannan peptide group. The mean liver weight in these two groups also had no difference, which indicated that CIS-A had no damage on the liver. However, the average tumor weight of the mice in the CIS-A group on the 14th day was 0.21 g (20 mg/kg), which was significantly lower than the tumor weight of mice in the negative control group (0.51 g) [Figure 3a]. Polysaccharide with high molecular in high concentration will lead to the aggregation of molecules, which will eventually affect the antitumor activity. However, the specific molecular mechanism needs further study.

Effects of CIS-A on tumor cell growth and apoptosis *in vitro*

L929 cells were stimulated with CIS-A (2.5, 5, 10, 20, and 40 μg/mL) for 24 h and detected by CCK-8 method. The results showed that polysaccharide CIS-A had a significant toxic effect on L929 cell line. The cell viability was significantly reduced after stimulated with different concentrations of CIS-A, as shown in Figure 3b and c. In comparison to control animals, when the concentration of CIS-A was 10 μg/mL and 20 μg/mL, L929 cells showed a significant cell survival of 82% and 69%, respectively. The OD value of L929 cells reached the maximum when

Table 2: Antitumor activities of CIS-A on S180 tumor (mean±standard deviation, *n*=6)

Group	Liver index (mg/g)	Spleen index (mg/g)	Thymus index (mg/g)		Average tumor weight (g)	Tumor inhibition rate (%)
			Left	Right		
S180-control	1.91±0.05	1.17±0.03	0.04±0.01	0.04±0.01	0.59±0.45	_
CIS-A	1.14±0.04$^{*,\#\#}$	1.184±0.24$^{*,\#\#}$	0.05±0.01	0.04±0.02	0.21±0.05$^{*,\#}$	64.4
Mannatide	2.01±0.22	1.15±0.20	0.04±0.01	0.04±0.01	0.19±0.09**	67.8

Significant differences from negative control group and positive control group were evaluated using Student's *t*-test: *As compared with control group, #As compared with mannatide group, $^{*,\#}P<0.05$, $^{**,\#\#}P<0.01$. S180-Control: Negative control group; CIS-A: Polysaccharide CIS-A group, 20 mg/kg; Mannatide: Positive control group of mannatide, 20 mg/kg. CIS-A: The polysaccharides from *Catathelasma imperiale* (Fr.) Sing

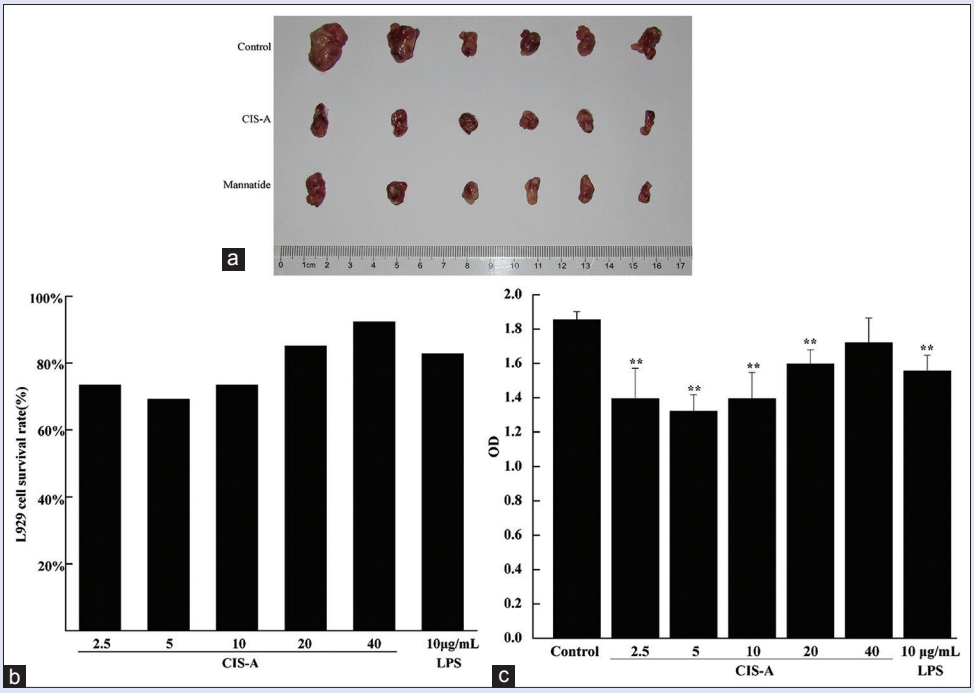

Figure 3: (a) Antitumor activity of *CIS-A in vivo*. Note – Control: Negative control group; *Catathelasma imperiale* (Fr.) Sing indicating *Catathelasma imperiale* (Fr.) Sing groups of 20 mg/kg; Man: Positive control group of mannatide. (b) Inhibition rate of L929 cells following CIS-A treatment *in vitro*, (c) absorbance of L929 cells treated with *CIS-A in vitro*

the concentration of CIS-A was 40 μg/mL. Thus, CIS-A displayed the inhibition of the proliferation of L929 cells.

Effect of CIS-A on T-cell activation *in vitro*

T-lymphocytes are referred to as T-cells. T-cells migrate from bone marrow hematopoietic stem cells into the thymus to differentiate and mature and become T-cells with immune activity. Mature T-cells can specifically bind to target cells, kill the target cells directly, or release the lymphatic factors, so that the immune effect is enhanced, which is mainly involved in the cellular immunity of organism. The stimulation of CIS-A on T-cells is shown in Figure 4b. Compared to the control group, the low concentration of CIS-A could significantly promote T-cell

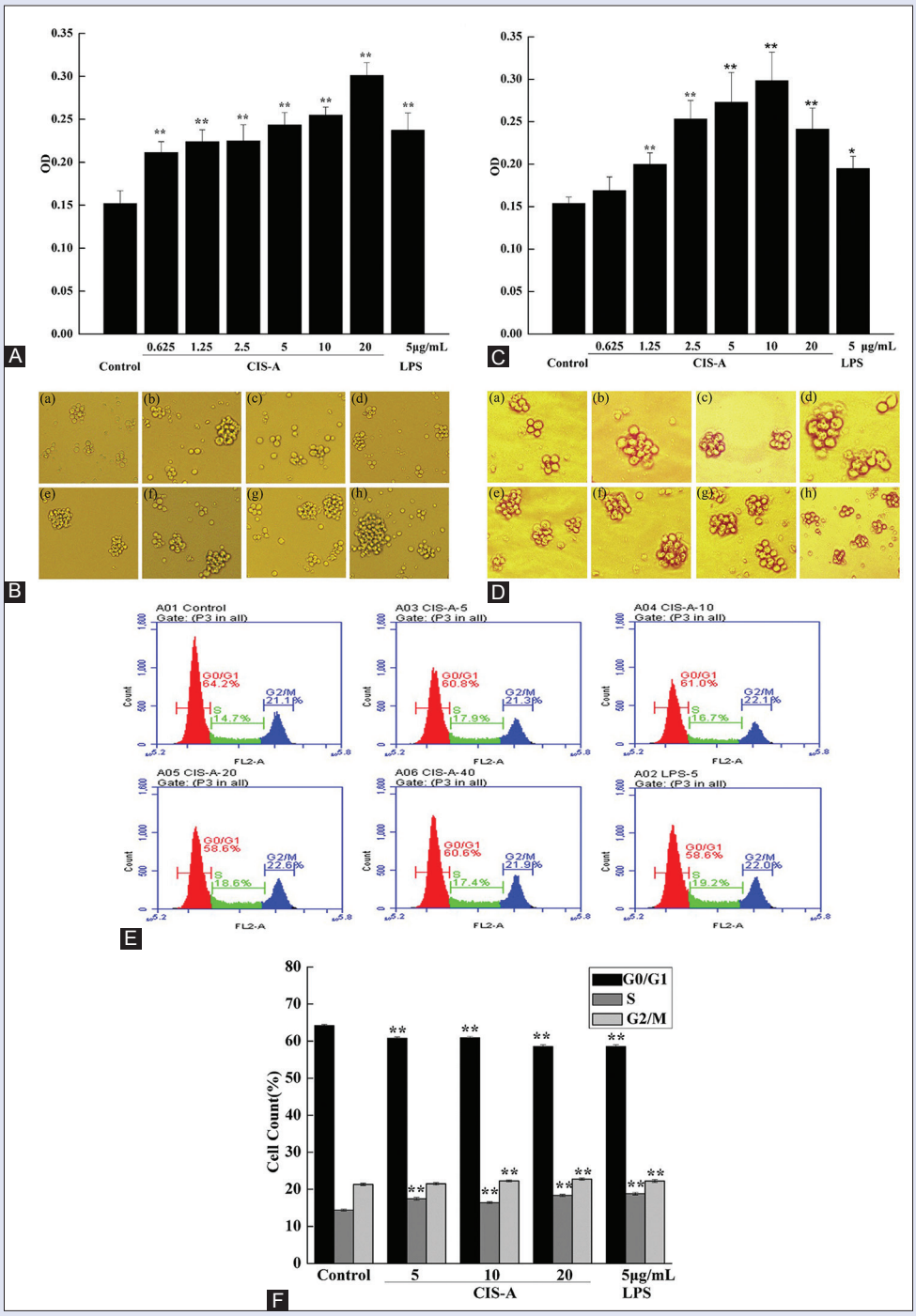

Figure 4: (A) The effect of CIS-A on the proliferation of T-cell, (B) the cell morphology effect of CIS-A on the proliferation of T-cell. Note – (a) is the blank group, (b) is the LPS group (5 μg/mL), (c-h) are the *Catathelasma imperiale* (Fr.) Sing experiment groups, cells treated with 0.625, 1.25, 2.5, 5, 10, 20 μg/mL *Catathelasma imperiale* (Fr.) Sing, respectively. (C) The effect of CIS-A on the proliferation of B-cell, (D) the cell morphology effect of CIS-A on the proliferation of B-cell. Note – (a) Is the blank group, (b) is the LPS group (5 μg/mL), (c-h) are the *Catathelasma imperiale* (Fr.) Sing experiment groups, cells treated with 0.625, 1.25, 2.5, 5, 10, 20 μg/mL *Catathelasma imperiale* (Fr.) Sing, respectively. (E) Effect on the cell cycle of B-cell by polysaccharide CIS-A, (F) statistical analysis of B-cell cycle

proliferation (0.625–20 μg/mL, $^{**}P < 0.01$), and the proliferation of T-cells was positively correlated with the concentration of CIS-A. Cell proliferation activity stimulated by 5 μg/mL CIS-A was comparable to or even greater than that stimulated by 5 μg/mL LPS, and the proliferation effect of T-cells reached the maximum value when the concentration of CIS-A was 20 μg/mL. The cell morphology of T-cells is shown in Figure 4a. Gradually, increasing the concentration of CIS-A, it could speed up cell division and increase cell volume. When 20 μg/mL of CIS-A was used to stimulate the T-cell, the T-cell clustered up most obviously.

Effect of CIS-A on B-cell activation *in vitro*

B-lymphocytes derived from bone marrow pluripotent stem cells, which can secrete antibodies, were the main medium of humoral immunity. When the concentration of CIS-A was 1.25–20 μg/mL, the cell proliferation of B-cells of CIS-A group differed from that of control group ($P < 0.01$) [Figure 4c]. The OD value of B-cells reached the maximum when the concentration of CIS-A was 10 μg/mL. From the morphological point of view, B-cells should be regular rounded and clustered. In this study, B-cell proliferation morphology is shown in Figure 4d. When B-cells were stimulated by CIS-A, they suspended in the culture bottle and grew in good condition, and the B-cell volume became larger.

Cell cycle is a process that from the beginning of cell division to the end of the next cell division. It includes cell interphase and cell division phase. Cells are dormant when they are in G0 phase. Cell interphase is divided into G1, S, and G2 phases. G1 phase is the synthesis period of RNA and ribosome; S phase is the synthesis period of DNA and histones; G2 phase is the mitosis preparation period when protein synthesis is completed. M phase is the cell division period. The results are shown in Figure 4e and f. The percentage of G0/G1 phase of B-cells in CIS-A group was less compared with blank control group. The percentage of G0/G1 phase was the lowest at 20 μg/mL. The percentage of cells in G2/M phase was positively correlated with the concentration of CIS-A, which indicated that the cell cycle of B-cells stimulated by CIS-A was decreased. It also indicated that G0 phase and the preparation time of G1 phase were decreased. The percentage of cells was increased in the period of G2 phase and cell division (M phase) and it could enhance the ability of B-cell division. In summary, CIS-A could be used as factor to promote B-cell proliferation by change cell cycle.

Effects of CIS-A on the proliferation of RAW264.7 cells *in vitro*

The antitumor activity of polysaccharides is the result of stimulating cell-mediated immune responses.[15] The results showed that CIS-A polysaccharide concentration group (0.625, 1.25, 2.5, 5, 10, and 20 μg/mL, $^{*}P < 0.05$; $^{**}P < 0.01$) could significantly promote the proliferation of RAW264.7 cells. When the concentration of CIS-A was 5 5 μg/mL, the proliferation of RAW264.7 cells was more obvious than 5 μg/mL LPS group ($P < 0.01$), as shown in Figure 5a. When the concentration of CIS-A increased to 10 and 20 g/mL, the values of OD were 0.78 and 0.70, respectively. The effect of proliferation was decreased significantly ($P < 0.05$).

Macrophage volume is large, and there was single nucleus; it is easy to observe. In this study, the morphology of macrophage proliferation is shown in Figure 5b. Under the stimulation of CIS-A, macrophages extended pseudopodia and split; when the number increased sharply, there would be overlapping.

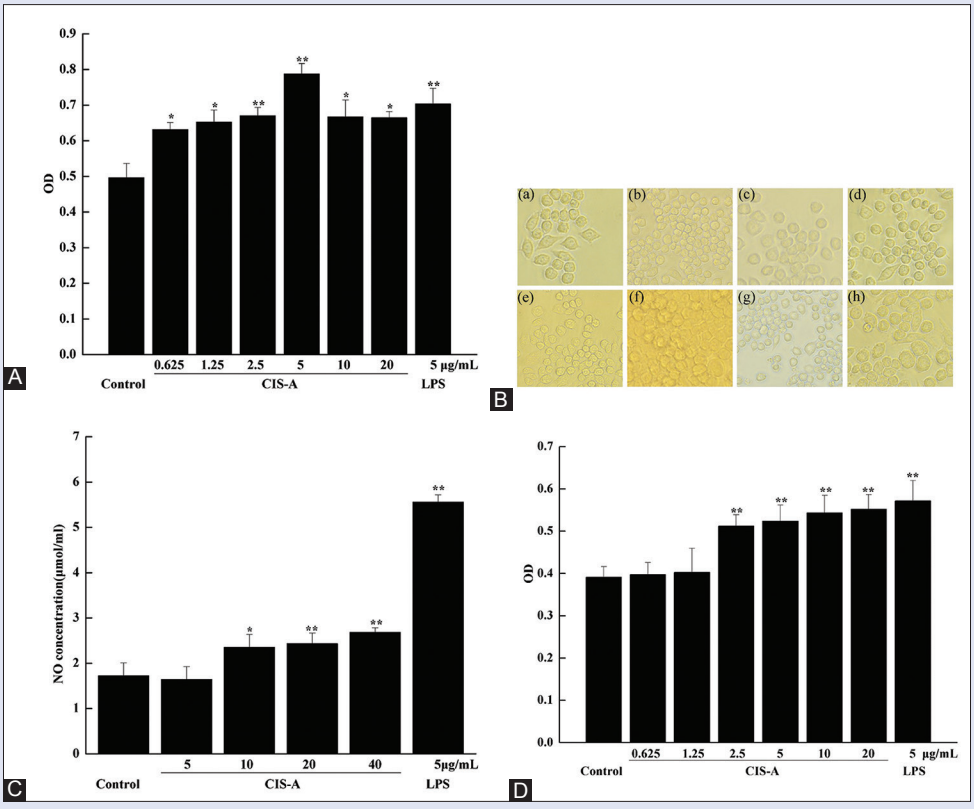

Figure 5: (A) The effect of CIS-A on the proliferation of RAW264.7 cells, (B) the cell morphology effect of CIS-A on the proliferation of RAW264.7 cells, Note – (a) Is the blank group, (b) is the lipopolysaccharide group (5 μg/mL), (c-h) are the CIS-A experiment groups, cells treated with 0.625, 1.25, 2.5, 5, 10, and 20 μg/ml CIS-A, respectively. (C) Production of NO in RAW264.7 cells stimulated by CIS-A, (D) the effect of CIS-A on the phagocytosis of RAW264.7 cells

Production of nitric oxide in RAW264.7 cells stimulated by CIS-A

Macrophage inflammation will produce a class of important free radicals, NO synthesis and release play host defense response and signal transfer function.[27] NO is very unstable, and it metabolized into nitrite (NO^{2-}) in the cell culture supernatant, so the concentration of NO^{2-} is determined by Griess method.[20] NO concentration (x, mol/mL) was used as the abscissa; the absorbance of A was used as the ordinate and drew the absorbance NO^{-} concentration curve. The linear regression equation was Y = 0.006X + 0.0464 and the correlation coefficient R^2 = 0.999. The results showed that the concentration of glucose in the range of 0–100 mol/mL was in good agreement with the Bill law. According to the standard curve, the concentration of NO released at different concentrations of CIS-A was calculated. When the concentration of CIS-A was 10 μg/mL, it could significantly stimulate the production of NO in RAW264.7 cells ($P < 0.05$). When the concentration of CIS-A in range of 20 and 40 μg/mL, CIS-A could significantly stimulate the production of NO in RAW264.7 cells ($P < 0.01$) and reached the maximum value when the concentration was 40 μg/mL [Figure 5c].

Effect of CIS-A on the phagocytic function of RAW264.7 cells

On the cell membrane of macrophages which have a variety of receptors, then the polysaccharide can stimulate macrophages. In this study, macrophage phagocytic activity was not significant at low concentration of CIS-A (0.625 and 1.25 g/mL). However, it is noteworthy that, compared with the control group, the concentration of CIS-A group can significantly promote the phagocytosis of mouse peritoneal macrophages [$P < 0.01$, Figure 5d] and it has a certain dose-dependent effect.

CONCLUSION

A new heteropolysaccharide was isolated from the fruiting bodies of *C. imperiale* (Fr.) Sing which had a molecular weight of 50486 Da. The structural feature analysis showed that the polysaccharide (CIS-A) was mainly composed of α-D-glucose and β-L-fucose. It had a backbone of three 1, 3-linked α-D-Glcp. There is a branch at the C2 of the polysaccharide backbone. The branches were mainly composed of two 2, 3-linked β-L-Fucp residue. Antitumor activity results showed that CIS-A could inhibit the growth of S180 tumor and promote the apoptosis of L929 cells. Immunoregulatory activity results showed that CIS-A could promote the proliferation of T-cells and promote B-cells by affecting G0/G1 phase, S phase, and G2/M phase. It also could promote the proliferation and phagocytosis of macrophages and induce cytokine release. This study provided scientific basis for the further study on the pharmacological action, structure–activity relationship, and more extensive application of fungal polysaccharide (CIS-A).

Financial support and sponsorship

This project was supported by the Science and Technology Support Project of Sichuan Province (2018JY0087 and 2018NZ0055), the Cultivate Major Projects of Sichuan Province (16CZ0018), the Nanchong science and Technology Bureau of Sichuan Province (16YFZJ0043), the Talent Program of China West Normal University (17YC328, 17YC136, 17YC329), the National Training Project of China West Normal University (17c039), and the Innovative Team Project of China West Normal University (CXTD2017-3).

Conflicts of interest

There are no conflicts of interest.

REFERENCES

1. Ferreira SS, Passos CP, Madureira P, Vilanova M, Coimbra MA. Structure-function relationships of immunostimulatory polysaccharides: A review. Carbohydr Polym 2015;132:378-96.
2. Lu L, Xiang D, Yiling H, Bo S, Daqun Z, Wanru H. Structural characterization and immunological activity of a novel heteropolysaccharide from *Lactikporus supharells* (Fr.) Murr. Lat Am J Pharm 2017;36:2386-96.
3. Ding X, Li J, Hou Y, Hou W. Comparative analysis of macrophage transcriptomes reveals a key mechanism of the immunomodulatory activity of *Tricholoma matsutake* polysaccharide. Oncol Rep 2016;36:503-13.
4. Zhu Y, Ding X, Wang M, Hou Y, Hou W, Yue C. Structure and antioxidant activity of a novel polysaccharide derived from *Amanita caesarea*. Mol Med Rep 2016;14:3947-54.
5. Ding X, Hou Y, Hou W, Zhu Y, Fu L, Zhu H. Structure elucidation and anti-tumor activities of water-soluble oligosaccharides from *Lactarius deliciosus* (L. Ex fr.) gray. Pharmacogn Mag 2015;11:716-23.
6. Ding X, Tang J, Cao M, Guo CX, Zhang X, Zhong J, *et al.* Structure elucidation and antioxidant activity of a novel polysaccharide isolated from *Tricholoma matsutake*. Int J Biol Macromol 2010;47:271-5.
7. Wang F, Hou Y, Ding X, Hou W, Song B, Wang T, *et al.* Structure elucidation and antioxidant effect of a polysaccharide from *Lactarius* camphoratum (Bull.) fr. Int J Biol Macromol 2013;62:131-6.
8. Hou Y, Ding X, Hou W, Zhong J, Zhu H, Ma B, *et al.* Anti-microorganism, anti-tumor, and immune activities of a novel polysaccharide isolated from *Tricholoma matsutake*. Pharmacogn Mag 2013;9:244-9.
9. Zhao D, Ding X, Hou Y, Hou W, Liu L, Xu T, *et al.* Structural characterization, immune regulation and antioxidant activity of a new heteropolysaccharide from *Cantharellus cibarius* fr. Int J Mol Med 2018;41:2744-54.
10. Ding X, Zhu H, Hou Y, Hou W, Zhang N, Fu L, *et al.* Comparative analysis of transcriptomes of macrophage revealing the mechanism of the immunoregulatory activities of a novel polysaccharide isolated from *Boletus speciosus* frost. Pharmacogn Mag 2017;13:463-71.
11. Ding X, Hou Y, Hou W. Structure feature and antitumor activity of a novel polysaccharide isolated from *Lactarius deliciosus* gray. Carbohydr Polym 2012;89:397-402.
12. Hou Y, Ding X, Hou W, Song B, Yan X. Structure elucidation and antitumor activity of a new polysaccharide from maerkang *Tricholoma matsutake*. Int J Biol Sci 2017;13:935-48.
13. Hou Y, Ding X, Hou W. Composition and antioxidant activity of water-soluble oligosaccharides from *Hericium erinaceus*. Mol Med Rep 2015;11:3794-9.
14. van Leeuwen SS, Kuipers BJH, Dijkhuizen L, Kamerling JP. Development of a (1)H NMR structural-reporter-group concept for the analysis of prebiotic galacto-oligosaccharides of the [β-d-galp-(1 → x)]n-d-glcp type. Carbohydr Res 2014;400:54-8.
15. Hou Y, Liu L, Ding X, Zhao D, Hou W. Structure elucidation, proliferation effect on macrophage and its mechanism of a new heteropolysaccharide from *Lactarius deliciosus* gray. Carbohydr Polym 2016;152:648-57.
16. Maity P, Nandi AK, Manna DK, Pattanayak M, Sen IK, Bhanja SK, *et al.* Structural characterization and antioxidant activity of a glucan from *Meripilus giganteus*. Carbohydr Polym 2017;157:1237-45.
17. Ding X, Hou Y, Zhu Y, Wang P, Fu L, Zhu H, *et al.* Structure elucidation, anticancer and antioxidant activities of a novel polysaccharide from *Gomphus clavatus* gray. Oncol Rep 2015;33:3162-70.
18. Liu L, Jia J, Zeng G, Zhao Y, Qi X, He C, *et al.* Studies on immunoregulatory and anti-tumor activities of a polysaccharide from *Salvia miltiorrhiza* bunge. Carbohydr Polym 2013;92:479-83.
19. Haneef J, Parvathy M, Thankayyan RS, Sithul H, Sreeharshan S. Bax translocation mediated mitochondrial apoptosis and caspase dependent photosensitizing effect of *Ficus religiosa* on cancer cells. PLoS One 2012;7:e40055.
20. Xiang D, Yiling H, Wanru H. Structure elucidation and antioxidant activity of a novel polysaccharide isolated from Boletus speciosus Forst, Int J Biol Macromol 2012; 50 (3): 613-8.
21. Zhang W, Huang J, Wang W, Li Q, Chen Y, Feng W, *et al.* Extraction, purification, characterization and antioxidant activities of polysaccharides from *Cistanche tubulosa*. Int J Biol Macromol 2016;93:448-58.
22. Zhang AQ, Liu Y, Xiao NN, Zhang Y, Sun PL. Structural investigation of a novel heteropolysaccharide from the fruiting bodies of *Boletus edulis*. Food Chem 2014;146:334-8.
23. Hou Y, Ding X, Hou W, Song B, Wang T, Wang F, *et al.* Immunostimulant activity of a novel polysaccharide isolated from *Lactarius deliciosus* (L. Ex fr.) gray. Indian J Pharm Sci

2013;75:393-9.

24. Komura DL, Ruthes AC, Carbonero ER, Gorin PA, Iacomini M. Water-soluble polysaccharides from *Pleurotus ostreatus* var. florida mycelial biomass. Int J Biol Macromol 2014;70:354-9.
25. Jing Y, Huang L, Lv W, Tong H, Song L, Hu X, *et al*. Structural characterization of a novel polysaccharide from pulp tissues of *Litchi chinensis* and its immunomodulatory activity. J Agric Food Chem 2014;62:902-11.
26. Cao W, Li XQ, Liu L, Yang TH, Li C, Fan HT, *et al*. Structure of an anti-tumor polysaccharide from *Angelica sinensis*, (Oliv.) Diels. Carbohyd Polym 2006;66:149-59.
27. Lee JS, Synytsya A, Kim HB, Choi DJ, Lee S, Lee J, *et al*. Purification, characterization and immunomodulating activity of a pectic polysaccharide isolated from Korean mulberry fruit Oddi (*Morus alba* L.). Int Immunopharmacol 2013;17:858-66.